

Charge-state dependence of InAs quantum-dot emission energies

S. Schulz, S. Schnüll, Ch. Heyn, and W. Hansen

Institute for Applied Physics, University of Hamburg, D-20355 Hamburg, Germany

(Received 18 July 2003; revised manuscript received 24 December 2003; published 28 May 2004)

The emission of electrons from self-assembled InAs quantum dots (SAQDs) is probed with transient capacitance spectroscopy (DLTS). The SAQDs are epitaxially grown on (100) GaAs and embedded in a slightly doped Schottky diode. Unprecedented resolution in our measurements enables us to determine different energies for emission from the s shell and the p shell of the quantum dots and to observe a strong field dependence of the activation energies derived from our DLTS spectra. Furthermore, we resolve different DLTS peaks for the emission from singly and doubly occupied s shells. The analysis of our data reveals that both the electric field as well as charge-state dependence of our spectra can be explained by a model in which phonon-assisted tunneling plays a crucial role for emission from the quantum-dot s state.

DOI: 10.1103/PhysRevB.69.195317

PACS number(s): 73.21.La, 73.23.Hk

I. INTRODUCTION

Self-assembled semiconductor quantum dots are intensively studied over the past few years since they represent artificial atomlike entities with intriguing quantum nature. These structures open up applications such as, e.g., low-threshold semiconductor lasers,¹ single-photon sources,² detectors for tunneling devices,³ and infrared detectors⁴. Self-assembled InAs quantum dots (SAQDs) are characterized by a strong three-dimensional quantum confinement of charge carriers provided by structural constraints, external fields, as well as by long-range strain fields. The effective confinement potential may have a complex structure, quite sensitive to growth parameters and material composition. On the other hand, a precise knowledge of the electronic level structure in the quantum dots is crucial for the above applications.

Valuable information on the electronic level structure can be provided by capacitance-voltage (CV) spectroscopy on dot layers incorporated in metal-insulator-semiconductor (MIS) devices⁵⁻⁷ or in Schottky diodes.^{8,9} In capacitance measurements on quantum dots in MIS diodes the interaction between charges in the dot and the reservoir are significant and clearly observed.¹⁰ Once an electron is injected from the contact into a dot, further charging is inhibited by the so-called Coulomb blockade as long as the contact potential is not readjusted. While capacitance spectra yield information on the level separation and the Coulomb charging energy, they do not provide direct information on the absolute binding energies of the dot states. In pure capacitance spectroscopy the measurement frequency is sufficiently low so that the electrons in the dots are always in equilibrium with the reservoir. In admittance spectroscopy the frequency is of the same order of or larger than the rate at which charge exchange with the quantum dots takes place. From the temperature dependence of the conductance signal, information of the quantum-dot electronic level structure has been derived.¹¹⁻¹³ The role of the Coulomb blockade energy, however, remained unclear.¹¹⁻¹³ Furthermore, in these experiments, the electric field at the quantum dots is determined by the doping of the diode and cannot be independently controlled in the experiment.

An alternative method to probe the energies of the elec-

tronic states in the quantum dots is deep level transient spectroscopy (DLTS), which has been very successfully applied for decades to investigate deep traps in semiconductors¹⁴ and more recently to SAQDs.¹⁵⁻¹⁹ Here, similar to ionization experiments on atoms, the emission of electrons from the quantum dots is probed. In contrast to capacitance measurements, the electron reservoir, from which the dots have been charged, is generally assumed to hardly play a role for the thermal electron emission from the dots. Furthermore, the electric field at the dots can be easily controlled with a bias in this experiment. It thus is very interesting to compare results of the two methods. The resolution of DLTS spectra published so far did not suffice to directly resolve the different energies for emission from the s and p levels or energy differences due to electron interaction. In the following, we will describe experiments with unprecedented resolution performed on optimized SAQDs ensembles. We are able to resolve the s - and p -shell emission and in addition we find significantly different rates for electron emission from the singly and doubly charged s state. Furthermore, we find a strong shift of the DLTS spectra with the electric field at the dots.

With a conventional Arrhenius analysis of the trap signature, we determine activation energies that are of the same order but slightly larger than those found for similar dots in DLTS and admittance spectroscopy measurements published previously.^{12,13,17,18} In previous work the activation energies were considerably lower than expected from comparison to theoretical predictions²⁰⁻²² and photoluminescence data. For an explanation of the low-energy values it was suggested that the emission takes place by thermal excitation to a single excited state bound to the quantum dot and a subsequent fast tunnel process. The latter process is thought to be so fast that it does not significantly contribute to the emission time. Thus the activation analysis of the experimental data would reveal the energy difference between the ground and the excited level. The strong field effect on the activation energies found in our experiments rules out an indirect process in which the thermal excitation to a single discrete level dominates the emission time. The change of the activation energies is even stronger than expected for the Poole-Frenkel effect that we

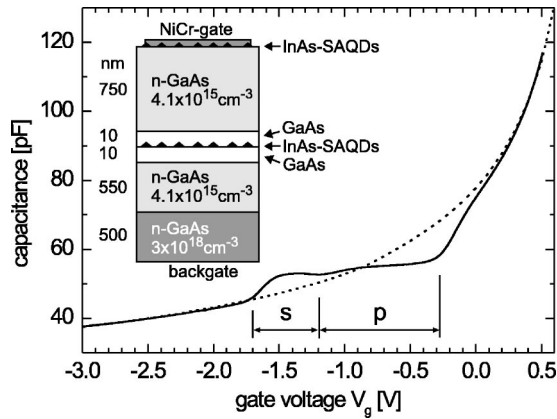


FIG. 1. Experimental CV trace of a Schottky diode for DLTS experiments with a layer of InAs SAQDs, taken at a temperature of 77 K and a frequency of 258 Hz. The dashed line is calculated for a Schottky diode without dots and otherwise identical layer structure. The inset depicts the layer structure of the diode.

can assume as an upper limit for any field effect on a bound level.

On the other hand it is well known from investigations of the field effect on the emission from deep impurity levels in bulk semiconductors^{23,24} that phonon-assisted tunneling may become very important. We analyze our data with a simple model,^{23,25} in which phonon-assisted tunneling through a band of energy states is responsible for the strong field effect.

II. SAMPLE PREPARATION

For the DLTS experiments the InAs SAQDs are embedded in slightly Si-doped GaAs Schottky diodes grown by molecular-beam epitaxy on semi-insulating (100) GaAs. The doping level of the Schottky diodes is kept very low in order to increase the resolution of the DLTS measurement and to reduce tunneling rates. The epitaxial layer sequence of a typical sample is depicted in the inset of Fig. 1. For inspection with atomic force microscopy (AFM), a second SAQD layer is grown on top of the sample. The AFM data show that our self-assembled InAs dots on (100) GaAs have a base width of about 30 nm and a height of about 6 nm. In total 12 samples with slightly different layer thicknesses and donor concentrations of the Schottky diode have been grown.

In the following we concentrate on results that have been obtained on two samples with effective donor concentration of 4.1 and $4.8 \times 10^{15} \text{ cm}^{-3}$. All the data presented here are from a Schottky diode with $4.1 \times 10^{15} \text{ cm}^{-3}$ donor density and a NiCr gate of 700 μm diameter. The layer thicknesses of the device are depicted in the inset of Fig. 1. The dot layer is located $d = 760 \text{ nm}$ below the gate. The dot density $N_{QD} = 2.1 \times 10^{10} \text{ cm}^{-2}$ was determined with AFM on a crystal piece taken from the wafer in the vicinity of the one used for preparation of the DLTS sample. Samples with higher donor concentration essentially yield qualitatively similar results. However, in the DLTS spectra the resolution becomes poorer and the p -emission peak is gradually dissolved by a tunneling background with increasing donor density.

Furthermore, two reference samples were grown contain-

ing no InAs dots. In the first reference sample only an InAs wetting layer was deposited. In the second reference sample no InAs was deposited at all. At a depth at which our other Schottky diodes contain the dot layer the growth of this sample was interrupted for a time equal to the InAs deposition time used in Schottky diodes with dots.

III. RESULTS

A. CV measurements

Figure 1 presents a CV trace of the Schottky diode. The trace was recorded at $T = 77 \text{ K}$ in order to ensure sufficiently fast charge exchange between SAQDs and electron reservoir at the modulation frequency of 258 Hz. On top of the overall Schottky-diode-type behavior of the CV trace we observe a plateaulike structure that reflects the charge accumulation in the dot layer. The capacitance value of the plateau corresponds well to the calculated value of 58 pF corresponding to the distance between dot layer and front gate of $d = 760 \text{ nm}$ and the gate area of $3.85 \times 10^{-3} \text{ cm}^2$ in this sample. Thus, at $-1.7 \text{ V} < V_g < -0.3 \text{ V}$ the depletion zone boundary traverses the SAQD layer. At closer inspection, a substructure is discernible in the plateau that we associate to the s -shell and the p -shell filling of the dots. Correspondingly, we expect that the s and p levels start to become occupied at $V_g = -1.7 \text{ V}$ and $V_g = -1.2 \text{ V}$, respectively. The arrows denote the gate voltage intervals at which two and four electrons are loaded into the dots, respectively. The intervals are calculated to 0.44 V and 0.88 V for two and four electrons per dot, assuming 760 nm distance between gate and quantum dots (Fig. 1) and a dot density $N_{QD} = 2.1 \times 10^{10} \text{ cm}^{-2}$ determined from AFM measurement. Our interpretation of the substructure is confirmed by the good correspondence between the interval lengths and the width of the structures, since we expect the SAQDs to accommodate two and four electrons in the s and p shell, respectively.

The reference sample without InAs shows a CV curve like the one calculated for a Schottky diode without dot layer. The reference sample containing only the InAs wetting layer shows a plateau with shorter length and no substructure. The plateau indicates that some charge is accumulated in the wetting layer.

B. DLTS measurements

In our DLTS experiments the SAQDs are charged by a voltage pulse applied across the Schottky diode that pushes the boundary of the depletion zone through the SAQD layer. The value of the filling-pulse voltage $V_g = V_p$ controls the charging state of the dots. After the filling pulse the gate voltage is reduced to a so-called reverse-bias value $V_g = V_r$, which lifts the dot levels above the Fermi energy of the contact. It is important to notice that now the charged dots are not in an equilibrium state. Thermal or tunnel emission will take place and the occupation of the dots decreases. Accordingly, the width of the depletion zone in the Schottky diode will slowly decrease, which is monitored by time-resolved capacitance measurements. The capacitance tran-

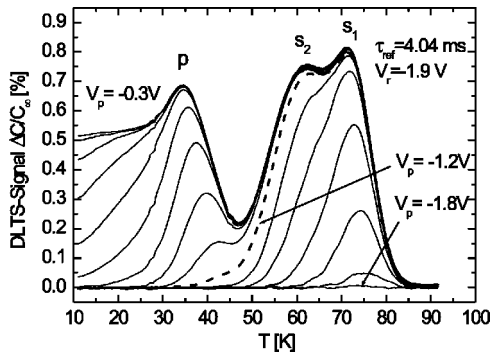


FIG. 2. DLTS-spectra of a Schottky diode with SAQDs. The reverse bias is set to $V_r = -1.9$ V. The pulse-bias values are increased from $V_p = -1.8$ V to $V_p = -0.3$ V in steps of 0.1 V. The trace recorded at $V_p = -1.2$ V is marked by a thick dashed line. Peaks associated to emission from s and p levels are marked by s_1 , s_2 , and p , respectively. The reference time is $\tau_{ref} = 4.04$ ms.

sient $C(t)$ recorded after the end of the filling pulse thus reflects the emission of the charge trapped in the dots. While the filling-pulse bias controls the occupation state of the dot at the beginning of the emission process, the reverse-bias value determines the electric field across the dots during the emission process and whether the new equilibrium state corresponds to partially filled or empty dots.

Figure 2 presents DLTS spectra of SAQDs recorded with different pulse-bias values ranging from -1.8 V to -0.3 V. The DLTS signal $\Delta C = C(t_2) - C(t_1)$ corresponds to the difference of the capacitance values recorded at two different delay times t_1 and t_2 after the filling pulse. In the figure the signal is normalized to the equilibrium capacitance C_∞ measured at $V_g = V_r$. As in conventional DLTS, it turns out that a specific emission process exhibits a DLTS-signal maximum at a temperature that depends on the two delay times. Both reference samples do not exhibit any DLTS signal in the range $10 \text{ K} < T < 300 \text{ K}$. This establishes that the peaks in Fig. 2 originate from the InAs quantum dots.

At a pulse bias $V_p = -0.3$ V clearly three different peaks are resolved in our spectra, which we associate to emission from quantum dots with fully occupied s and partly occupied p shell, respectively. The peaks in the DLTS spectra are denoted s_1 , s_2 , and p , correspondingly. The identification of the emission processes is confirmed by comparison of the pulse biases, at which the peaks arise, with the gate-voltage values in the CV traces, at which we expect occupation of the s and p shell. According to the CV trace at $V_g = -1.8$ V no dots should be occupied. Indeed in the DLTS measurement no peaks are observed at the corresponding filling-pulse value. The peak denoted by s_1 just arises at $V_p = -1.7$ V as expected from the CV trace. Furthermore, the peak associated to emission from the p level arises at $V_g = -1.2$ V, where the minimum in the substructure of the plateau in the CV trace is located. Interestingly, before the p peak emerges, a peak denoted s_2 appears close to the s_1 peak which has similar strength and has a maximum position located at slightly lower temperature. We associate this peak to the emission from the two-electron state in the s shell. We note that, with increasing filling of the p shell, tunneling

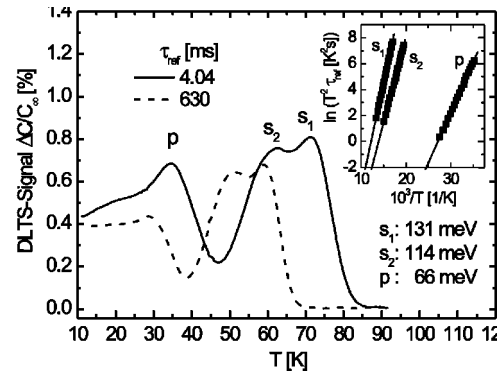


FIG. 3. DLTS spectra recorded at two different reference times as denoted. Inset: Arrhenius plots of the emission rates determined from the maximum positions of the DLTS spectra for many different reference times. The activation energies are determined from the slopes of a linear fit to the data (straight lines). The activation energies for emission from s and p states are s_1 , 131 meV, s_2 , 114 meV, p , 66 meV.

processes become important, which cause a temperature-independent background at low temperatures ($T < 30$ K). This behavior, indicating that the thermal excitation becomes slower than the tunnel emission at these temperatures, has been observed in previous DLTS experiments as well.¹⁸

IV. DISCUSSION

Usually, DLTS spectra of InAs quantum dots have been evaluated with a model, in which an activation energy E_a is determined from the temperature dependence of the emission rate with an Arrhenius analysis. In this model it is assumed that, at temperatures close to the peaks, the capacitance transients are dominated by the emission from one level and thus can be described by a single emission rate e_n : $C(t) = C_\infty - \Delta C_0 \exp(-e_n t)$. In this case the emission rate at the maxima in the DLTS spectra is given by $e_n = \tau_{ref}^{-1}$, where $\tau_{ref} = (t_2 - t_1) / \ln(t_2/t_1)$ is the so-called reference time.¹⁴ The dots are regarded as deep traps that can be discharged only by a thermal-activated process such as, e.g., excitation to the continuum of the barrier. Such a process is described by an emission rate $e_n(T) = \sigma_n \gamma T^2 \exp(-E_a/kT)$, where σ_n is the capture cross section, γ is a temperature independent constant, k the Boltzmann constant, and E_a is an apparent barrier height. In the simple case of emission by thermal excitation from the dot ground state to the continuum E_a corresponds to the binding energy of the ground state. In the case of more complex scenarios E_a may deviate from this energy. Indirect emission processes have been proposed that involve a thermal excitation to a bound dot level and a subsequent tunnel process.^{12,13,17,18} Neglecting the tunnel time, above analysis can still hold if E_a now is identified with the separation between the ground and the excited state.

The emission rates $e_n(T)$ are obtained from measurements taken with different reference times. In the inset of Fig. 3 the thus determined emission rates are depicted in a so-called trap signature, i.e., a logarithmic plot of the emission rates, which accounts for the quadratic temperature de-

pendence of the prefactor.^{14,16,17} The activation energies E_a are obtained from the slopes of the data. The s_1 , s_2 , and p peaks yield the activation energies 131 meV, 114 meV, and 66 meV, respectively. Obviously, the activation energies of the quantum dots very sensitively depend on the charge state.

One might expect that the differences of the excitation energies simply reflect the energy-level distances assuming the state into which the trapped electrons are excited is identical in all three cases. Indeed, a comparison of our activation energy differences with the results of *CV* measurements on very similar InAs SAQDs incorporated in undoped MIS devices gives amazing coincidence. Such devices have been grown just prior or after the growth of the Schottky diodes for the DLTS experiments with identical parameters for the InAs dot formation. Due to the absence of dopants in the MIS diodes, the charging peaks associated to the s_1 , s_2 , and p levels are well resolved in such kind of device.^{5,7} A simple analysis of the *CV* traces from our MIS diodes yields a Coulomb charging energy of 17 meV for injection of the second electron into the s level and an energy separation of 50 meV between s and p levels. These values are very close to DLTS data differences of the s_1 and s_2 activation energies of 17 meV and the s_2 and p activation energies of 48 meV, determined from the data in Fig. 3.

However, one should be very careful in directly comparing these energies. Indeed the coincidence is very surprising. We actually do not expect the Coulomb charging energy of the *CV* measurements to be directly related to the differences of the activation energies observed in the DLTS spectra. It is presently understood that the charging energy, which is responsible for the splitting of the s -level peak in the *CV* measurements of MIS diodes, is dominated by the Coulomb blockade energy.^{5,7} It corresponds to the charging energy of a metallic capacitor that has the shape and size of the dot and is related to the rise of the electrical potential difference between the dot and the electrodes when the dot is charged. Since the emission process in the DLTS measurement is based on a local excitation, e.g., to the barrier surrounding the dot or to an excited state within the dot, it should be less affected by such potential changes.

It is important to note that while according to above argument the potential difference between the back contact and the dot levels should not affect the activation energy, the electric field F across the dot does. In our experiments, we control the field across the dots by the reverse bias. Filled symbols in Fig. 4 mark activation energies obtained from an Arrhenius analysis of the DLTS data at different reverse-bias voltages. The mean electric field across the dots is calculated analytically from the reverse-bias value V_r , the doping of the diode, the charge state of the dots, and the dot density of $N_{QD} = 2.1 \times 10^{10} \text{ cm}^{-2}$. The contribution of the charge in the dots to the total electric field is estimated by the field of a homogeneous two-dimensional charge distribution with density according to the dot density and the charge state of the dot.

The activation energies considerably decrease with increasing electric field. In order to conceive the strength of the field effect we may first consider the strength that would be expected for the Poole-Frenkel effect^{16,26} in our quantum

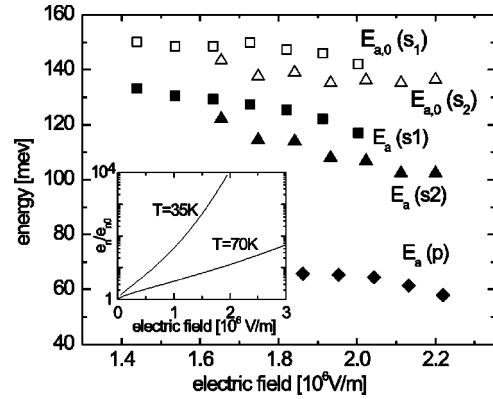


FIG. 4. Activation energies as function of the electric field at the dots calculated from the reverse bias and the charge state of the dots before emission. Data points marked with filled symbols have been obtained from standard Arrhenius analysis. Data points marked with open symbols are calculated using Eq. (1) for enhanced emission rates due to phonon-assisted tunneling. The inset shows two plots from Eq. (1) for a trap with $E_{a,0} = 150$ meV for the 70 K curve and with $E_{a,0} = 100$ meV for the 35 K curve.

dots. Assuming a square-well confinement of width Δz in field direction the emission energy is reduced by the electric field F by an amount of $qF\Delta z/2$, where q is the electron charge. According to the data of Fig. 4 the extension Δz of the square well would have to be 52 nm in order to explain the electric-field dependence of the energies. This extension is much larger than the structural dot heights of typical 6 nm determined by AFM. We thus conclude that the strong field dependence observed in our experiments cannot be explained by the Poole-Frenkel effect. Furthermore, we note that the field dependence of the binding energy of a level bound to the quantum dot is expected to be even smaller than the value estimated by the Poole-Frenkel effect. Thus the models suggested in previous publications, in which the measured activation energies are associated to thermal excitation from the ground state to a single excited quantum-dot state, do not explain our findings.

It is well known from experiments devoted to the electric-field dependence of the emission rate from deep impurity states in semiconductors, such that strong field dependence of the emission rate occurs, whenever phonon-assisted tunneling becomes important.^{23–25,27} Data on the field dependence of the emission rates from deep centers in GaAs were understood with a model in which the escape from the trap was considered to be a two-step process comprising a phonon absorption and a subsequent tunnel process from higher energies where the tunnel probability is more favorable. The strong field dependence arises from the field dependence of the tunnel process.²⁸ Different models have been proposed for the phonon coupling in the work of Vincent²³ and Makram-Ebeid.^{24,27} For an estimate we favor the model by Vincent,²³ since it contains less open parameters. Furthermore, we note that the presence of a band of wetting-layer states at energies close to the continuum may render this model a good description. We assume the electrons to be bound by a one-dimensional square well with only a single bound state in order to keep the model simple. The emission

rate is given by an integral summing the contributions from all indirect processes involving virtual states at energies $0 < E < E_{a,0}$:

$$\frac{e_n}{e_{n,0}} = 1 + \int_0^{E_{a,0}/kT} \exp\left(z - z^{3/2} \frac{(8m^*)^{1/2}(kT)^{3/2}}{3q\hbar F}\right) dz, \quad (1)$$

where $E_{a,0}$ is the binding energy of the ground state and F the electric field in the barrier estimated as above. The effective mass $m^* = 0.07m_e$ is chosen to be close to the GaAs conduction-band mass. The rate $e_{n,0} \propto T^2 \exp(-E_{a,0}/kT)$ is the emission rate that would be measured in the absence of phonon-assisted tunneling. Here we neglect the Poole-Frenkel effect on the binding energy. It can be easily incorporated into the model²⁵ but turns out to yield only small corrections in the case of our InAs quantum dots. Employing a one-dimensional model is expected to overestimate the field effect.²⁵ On the other hand the fields estimated by a homogeneous charge distribution are lower than those in close distance to the dots. We note that in our case Eq. (1) can be analytically approximated by²³

$$\frac{e_n}{e_{n,0}} = \frac{2\pi^{1/2}}{(kT)^{3/2}} \frac{q\hbar F}{(8m^*)^{1/2}} \exp\left[\frac{1}{3(kT)^3} \frac{(q\hbar F)^2}{8m^*}\right], \quad (2)$$

which shows that the values of the integral are only very weakly dependent on the upper boundary $E_{a,0}$. In our model the integral can thus easily be evaluated so that from the measured emission rates e_n we can calculate the rates $e_{n,0}$ that yield the binding energy of the ground state in an Arrhenius analysis.

The thus determined binding energies of the ground level are close to 150 meV and show a weak electric-field dispersion. They are depicted in Fig. 4. We note that due to the highly nonlinear character of the tunneling process the measured emission rates very strongly depend on the electric field. Thus our estimate of the contribution of the dot charge to the electric field in the barrier may be too coarse. In view of the roughly estimated electric fields the differences in the emission rates of quantum dots charged with one and two electrons, respectively, indeed may be explained by differences in the tunneling rates according to the different fields in the barrier alone.

Finally, we note that we find in samples with stronger doping the resolution of the emission peaks from the singly and doubly charged quantum dots to be always poorer. This may be easily explained as follows. The minimum electric field present at the dots during the reverse bias in the DLTS experiment linearly increases with the doping. Thus the relative change of the fields associated to dots occupied with one and two electrons becomes smaller. Accordingly, the emission rates approach each other.

The p -level maximum is superimposed on a background arising from tunnel emission that becomes important at low temperatures and thus at low emission energies.¹⁸ This limits the precision at which the field effect of the p -level emission energy can be determined. In the inset of Fig. 4 the enhancement of the emission rates by the phonon-assisted tunneling process with respect to the emission by pure thermal excita-

tion are plotted. The parameters of the two traces are chosen close to those of our experiment for emission from the s and the p state, respectively. For example, at a field $F = 2 \times 10^6$ V/m and a temperature $T = 70$ K the rate is enhanced by factor 12.5 for emission from the s state. Obviously, the enhancement is considerably stronger for emission from the p state rendering the field effect even more important in this case. Estimating $E_{a,0} = 100$ meV for the p state appearing at 35 K in the DLTS spectra and assuming a field of 2×10^6 V/m the emission rate is enhanced by a factor 10^4 . At present the precision of the data does not suffice to calculate reliable values for the p -state binding energies according to the phonon-assisted tunneling model (see inset of Fig. 4).

In the following we would like to discuss the shift of the maximum in the DLTS spectrum when the electric field is changed while the reference time is kept constant. Neglecting nonexponential terms and with the help of Eq. (2) we can calculate the shift of the maximum in the DLTS spectrum with electric field expected according to the phonon-assisted tunneling model:

$$\frac{\delta T_{\max}}{\delta F} = \frac{2}{3} \frac{T_{\max}}{F} \left(1 - \frac{8m^* E_{a,0} (kT_{\max})^2}{(q\hbar F)^2}\right)^{-1}. \quad (3)$$

Assuming a ground-state binding energy of $E_{a,0} = 150$ meV we obtain $\delta T_{\max}/\delta F = -1.9$ K $(10^6$ V/m) $^{-1}$ at parameters chosen according to our experiment, i.e., $T = 70$ K and $F = 1.5 \times 10^6$ V/m.

Alternative to the above model one might suggest an indirect emission process involving thermal activation to a single resonant dot state and subsequent tunneling. Such a process has been previously suggested to explain experimental data but without considering the influence of the tunneling process to the emission rate.^{12,13,17} We expect quite different electric-field dependencies for phonon-assisted tunneling via a band of states and an escape process, in which only one excited dot state is involved. In the case of tunnel emission from a single resonant dot state we assume an emission rate according to

$$e_n \propto \exp\left(-\frac{\Delta E}{kT}\right) \exp\left(-\frac{4}{3} \frac{\sqrt{2m^*} E_a^{3/2}}{q\hbar F}\right), \quad (4)$$

where the first term corresponds to thermal excitation from the ground state to the excited state at energy ΔE above the ground state and the second term describes the field-induced tunneling through a barrier of apparent height E_a . Thus for the field dependence of the temperature at which the DLTS maximum occurs we expect

$$\frac{\delta T_{\max}}{\delta F} = -\frac{4}{3} \left(\frac{T_{\max}}{F}\right)^2 \frac{\sqrt{2m^*} k E_a^{3/2}}{q\hbar \Delta E}. \quad (5)$$

With values $\Delta E = 50$ meV, $E_a = 100$ meV, and parameters m^* , T , and F chosen as above we obtain $\delta T_{\max}/\delta F = -220$ K $(10^6$ V/m) $^{-1}$, which is two orders of magnitude larger than the value estimated with our tunneling model. The shifts of the DLTS maxima observed in our experiments

are $\delta T_{\max}/\delta F = -4 \text{ K} (10^6 \text{ V/m})^{-1}$ and thus close to the values calculated from our model, Eq. (3).

The different behavior of both models originates from two facts. First, in the phonon-assisted tunneling model the emission takes place from a band located around an energy, where the integrand in Eq. (1) is maximal. The width and location of the energy band contributing to the emission rate depends on the electric field. This in essence causes the field dependence of the activation energy and explains why the shifts of the DLTS maximum in Eqs. (3) and (5) are different. Second, if thermally assisted tunneling would take place through a single discrete state at the values used for above estimates, the electron has to transit through a relatively large tunnel barrier of about 100 meV height. In contrast the maximum of the integrand in Eq. (1) is located at an energy of about 9 meV below the free continuum energy. This means that in the phonon-assisted tunneling model the effective tunnel barrier is drastically lower, resulting in a smaller shift of the DLTS maximum.

Photoluminescence measurements on quantum-dot samples of the same wafer as the one used for this experiment show at $T=77 \text{ K}$ a luminescence line at energy $E_{ss} = 1.099 \text{ eV}$ which is believed to arise from recombination of s -level electrons with s -level holes. At higher excitation intensity a second peak occurs at $E_{pp} = 1.159 \text{ eV}$, which we associate to recombination of p -level electrons and holes. The luminescence energies hardly depend on the voltage applied at the Schottky diode, which can be taken as an evidence that the dot levels hardly change in the fields applied. Neglecting exciton binding energies the difference to the GaAs bulk luminescence of 1.507 eV should account for both the binding energies of the electron as well as hole ground level in the dot. In order to determine the latter we have performed optically excited DLTS measurements. Here the capacitance transients are recorded after excitation with a pulse of an infrared light emitting diode emitting at $\lambda = 950 \text{ nm}$. A strong DLTS signal is observed from which we determine a hole binding energy of 160 meV at low illumination intensity with a conventional Arrhenius analysis of the emission rates. This energy is very similar to values reported in previous publications.^{13,18} From the luminescence energies and the hole level binding energy we determine an electron binding energy of 248 meV, which is of the same order as found for electron states in InAs dots by other authors.^{12,18} On the other hand it is significantly larger than the electron binding energy determined from our DLTS analysis. The discrepancy remains to be resolved and may be understood as an indication that possibly more refined models are needed, which, e.g., include temperature-dependent capture rates,²⁹

the realistic phonon spectrum at the dot site,²⁷ and include resonant excited states. Furthermore, it presently is not clear, whether for the emission of the considerably heavier holes phonon-assisted tunneling is also important. The values derived here for the electron and hole energies are well within the range predicted by eight-band $\mathbf{k}\cdot\mathbf{p}$ calculations^{21,22} or multiband pseudopotential calculations,³⁰ taken the uncertainty with which dot geometry and composition are known.

V. SUMMARY

In summary, in optimized Schottky diodes containing InAs SAQDs, we obtain DLTS spectra in which separate maxima associated to the emission from the s and the p shell of the dots are resolved. Furthermore, the spectra exhibit different peaks for electron emission from the singly and doubly occupied s shell. The emission processes are identified by the pulse-bias dependency and comparison with capacitance-voltage traces. The reverse bias applied during sampling of the capacitance transient is used to control the electric field across the dots during the emission process. Activation energies are derived from a conventional Arrhenius analysis of the experimental emission rates. They are found to be clearly different for emission from the singly and doubly occupied s state. Our results demonstrate that the charge state of the dots strongly influences the emission process. Furthermore, we find that the activation energies show a very strong electric-field dependence. From the field dependence we infer that the electrons escape from the dots by phonon-assisted tunneling processes. We analyze our DLTS data within a simple model that accounts for phonon-assisted tunneling. While the conventional analysis of our DLTS data yields an activation energy of typically 130 meV for emission from the singly occupied s state, an energy of 150 meV is found after correction for the phonon-assisted tunnel process. The different activation energies determined from the conventional analysis of our data for emission from the singly and doubly occupied s state may be due to the different electric fields in the barrier alone. Finally, we note that we expect the field dependence of the emission rates to be more important in samples with higher doping leading to large corrections to the emission energies since there the inevitable fields are larger.

ACKNOWLEDGMENTS

We profited from discussions with A. Rack and M. Tews. We thank L. Karsten for photoluminescence measurements. This work was supported by the Deutsche Forschungsgemeinschaft via Grant No. SFB 508 "Quantenmaterialien."

¹D. Bimberg, M. Grundmann, and N. Ledentsov, *Quantum Dot Heterostructures* (Wiley, New York, 1999).

²E. Moreau, I. Robert, J. Gerard, I. Abram, L. Manin, and V. Thierry-Mieg, *Appl. Phys. Lett.* **79**, 2865 (2001).

³I.E. Itskevich, T. Ihn, A. Thornton, M. Henini, T.J. Foster, P. Moriarty, A. Nogaret, P.H. Beton, L. Eaves, and P.C. Main, *Phys.*

Rev. B **54**, 16 401 (1996).

⁴S.W. Lee, K. Hirakawa, and Y. Shimada, *Appl. Phys. Lett.* **75**, 1428 (1999).

⁵H. Drexler, D. Leonard, W. Hansen, J.P. Kotthaus, and P.M. Petroff, *Phys. Rev. Lett.* **73**, 2252 (1994).

⁶G. Medeiros-Ribeiro, J.M. Garcia, and P.M. Petroff, *Phys. Rev. B*

- 56**, 3609 (1997).
- ⁷B.T. Miller, W. Hansen, S. Manus, R.J. Luyken, A. Lorke, J.P. Kotthaus, S. Huant, G. Medeiros-Ribeiro, and P.M. Petroff, *Phys. Rev. B* **56**, 6764 (1997).
- ⁸P.N. Brunkov, A. Polimeni, S.T. Stoddart, M. Henini, L. Eaves, P.C. Main, A.R. Kovsh, Y.G. Musikhin, and S.G. Konnikov, *Appl. Phys. Lett.* **73**, 1092 (1998).
- ⁹R. Wetzler, A. Wacker, E. Schll, C.M.A. Kapteyn, R. Heitz, and D. Bimberg, *Appl. Phys. Lett.* **77**, 1671 (2000).
- ¹⁰R.J. Warburton, B.T. Miller, C.S. Dürr, C. Bödefeld, K. Karrai, J.P. Kotthaus, G. Medeiros-Ribeiro, P.M. Petroff, and S. Huant, *Phys. Rev. B* **58**, 16 221 (1998).
- ¹¹S.K. Zhang, H.J. Zhu, F. Lu, Z.M. Jiang, and X. Wang, *Phys. Rev. Lett.* **80**, 3340 (1998).
- ¹²W.-H. Chang, W.Y. Chen, M.C. Cheng, C.Y. Lai, T.M. Hsu, N.-T. Yeh, and J.-I. Chyi, *Phys. Rev. B* **64**, 125315 (2001).
- ¹³W.-H. Chang, W.Y. Chen, T.M. Hsu, N.-T. Yeh, and J.-I. Chyi, *Phys. Rev. B* **66**, 195337 (2002).
- ¹⁴D.V. Lang, *J. Appl. Phys.* **45**, 3023 (1974).
- ¹⁵S. Anand, N. Carlsson, M.-E. Pistol, L. Samuelson, and W. Seifert, *Appl. Phys. Lett.* **67**, 3016 (1995).
- ¹⁶S. Anand, N. Carlsson, M.-E. Pistol, L. Samuelson, and W. Seifert, *J. Appl. Phys.* **84**, 3747 (1998).
- ¹⁷C.M.A. Kapteyn, F. Heinrichsdorff, O. Stier, R. Heitz, M. Grundmann, N.D. Zakharov, P. Werner, and D. Bimberg, *Phys. Rev. B* **60**, 14 265 (1999).
- ¹⁸C.M.A. Kapteyn, M. Lion, R. Heitz, D. Bimberg, P. Brunkov, B.V. Volovik, S.G. Konnikov, A.R. Kovsh, and V.M. Ustinov, *Appl. Phys. Lett.* **76**, 1573 (2000).
- ¹⁹V.V. Ilchenko, S.D. Lin, and C.P. Lee, *J. Appl. Phys.* **89**, 1172 (2001).
- ²⁰M. Grundmann, O. Stier, and D. Bimberg, *Phys. Rev. B* **52**, 11 969 (1995).
- ²¹C. Pryor, *Phys. Rev. B* **57**, 7190 (1998).
- ²²O. Stier, M. Grundmann, and D. Bimberg, *Phys. Rev. B* **59**, 5688 (1999).
- ²³G. Vincent, A. Chantre, and D. Bois, *J. Appl. Phys.* **50**, 5484 (1979).
- ²⁴S. Makram-Ebeid and M. Lannoo, *Phys. Rev. Lett.* **48**, 1281 (1982).
- ²⁵P.A. Martin, B.G. Streetman, and K. Hess, *J. Appl. Phys.* **52**, 7409 (1981).
- ²⁶J.L. Hartke, *J. Appl. Phys.* **39**, 4871 (1968).
- ²⁷S. Makram-Ebeid and M. Lannoo, *Phys. Rev. B* **25**, 6406 (1982).
- ²⁸E.N. Korol, *Fiz. Tverd. Tela (Leningrad)* **19**, 2266 (1977) [*Sov. Phys. Solid State* **8**, 1327 (1977)].
- ²⁹O. Engström (private communication).
- ³⁰A.J. Williamson, L.W. Wang, and A. Zunger, *Phys. Rev. B* **62**, 12 963 (2000).